Electronic Supplementary Information (ESI)

Mimicking Enzymatic Systems: Modulation of the Performance of Polymeric Organocatalysts by Ion-Specific Effects

Yun Xu,[a] Zan Hua,[a] Jian Zhang,[a] Jun Yang,[a] Zhonglin Cao,[a] Dongyang Zhang,[a] Lingxin He,[a] Vincent S. J. Craig,[c] Guangzhao Zhang,[b] Guangming Liu*[a]

[a]Department of Chemical Physics, Hefei National Laboratory for Physical Sciences at the Microscale, University of Science and Technology of China, Hefei, P. R. China 230026.
[b]Faculty of Materials Science and Engineering, South China University of Technology, Guangzhou, P. R. China 51064.
[c]Department of Applied Mathematics, Research School of Physics and Engineering, The Australian National University, Canberra, ACT 0200, Australia.

Contents

Materials and Methods

Materials. N,N-Diethylacrylamide (DEA, 98%, TCI) was distilled under a reduced pressure over CaH_2. trans-4-Hydroxy-L-proline (99%), 3-aminopropyltriethoxysilane (APTES, 99%), 1-ethyl-3-(3-dimethylaminopropyl)carbodiimide hydrochloride (EDC, 98.5%), 4-dimethylaminopyridine (DMAP, 99%) were purchased from Aladdin and used as received. 4,4'-Azobis(isobutyronitrile) (AIBN) was recrystallized three times from ethanol. 4-Nitrobenzaldehyde (98%) was purchased from Sigma-Aldrich and used as received. Cyclohexanone (99.0%, Sigma-Aldrich) was distilled under a reduced pressure over $KMnO_4$. Dimethyl sulfoxide (DMSO) and dichloromethane (DCM) were refluxed in the presence of CaH_2, and then distilled prior to use. Toluene was refluxed in the presence of Na wire, and then distilled prior to use. The water used was purified by filtration through the Millipore gradient system after distillation, giving a resistivity of 18.2 MΩ cm. The silicon (100) wafers were purchased from Wafer Works Corporation (Shanghai, China). The chain transfer agent, S-1-dodecyl-S′-(R,R′-dimethyl-R″-acetic acid) trithiocarbonate, was synthesized according to a previously described procedure.[S1]

Characterizations. All proton nuclear magnetic resonance (^{1}H NMR) spectra were recorded on a Bruker AV400 NMR spectrometer. Fourier transform infrared (FT-IR) spectra were recorded on a Bruker VECTOR-22 IR spectrometer with a spectral resolution of 4 cm^{-1}. Transmission electron microscope (TEM) measurements were conducted on a Philips CM 120 electron microscope at an acceleration voltage of 100 kV. The sample for TEM measurements was prepared by placing 10 μL of solution containing nanoparticles on copper grids, successively coated with thin films of Formvar and carbon. The contact angle measurements were performed using a KSV (Helsinki, Finland) CAM 200 contact angle goniometer and the thickness of the grafted polymer layer on the silica surface was determined by spectroscopic ellipsometry (M2000V, J. A. Woollam, U.S.A.) at two incident angles of 65° and 75°. HPLC analysis was performed on Waters-Breeze (2487 Dual λ Absorbance Detector and 1525 Binary HPLC Pump). The hydrodynamic radius (R_h) of the polymer-grafted nanoparticles was

determined by using a commercial laser light scattering spectrometer (ALV/DLS/SLS-5022F) at a scattering angle of 90°.

Synthesis of *O*-Acryloyl-*trans*-4-hydroxy-L-proline hydrochloride.[S2] *trans*-4-Hydroxy-*L*-proline (9.5 g, 72.7 mmol) was dried at 65 °C for 24 h and then added in portions within 3 min to a round bottom flask containing CF_3CO_2H (22 mL) with vigorous stirring in an ice/water bath. CF_3SO_3H (0.75 mL, 8.5 mmol) was added to the solution after 5 minutes of reaction. After an additional 5 minutes, acryloyl chloride (11.5 mL, 142.2 mmol) was added to the solution. The reaction mixture was stirred for an additional 2 h at room temperature. Then, the reaction flask was cooled with an ice/water bath, followed by the addition of Et_2O (135 mL) with vigorous stirring. The resulting white solid was vacuum-filtered and washed with additional Et_2O (100 mL) two times and dried under vacuum at room temperature. The successful synthesis of O-Acryloyl-trans-4-hydroxy-L-proline was confirmed by ^{1}H NMR (400MHz, D_2O):δ(ppm) 2.38-2.68 (m, 2H), 3.57-3.7 (m, 2H), 4.52-4.63 (m, 1H), 5.52 (s, 1H), 5.95-4.63 (dd, 2H), 6.10-6.17 (m, 1H).

Synthesis of functionalized silica nanoparticles. Silica nanoparticles with uniform size and morphology were prepared by the Stöber method.[S3] The introduction of amine groups on the surface of silica nanoparticles was achieved by reaction of aminopropyl trimethoxysilane with the silanol groups on the particle surface. Afterwards, amino-functionalized silica nanoparticles (2.0 g) were dispersed in CH_2Cl_2 (40.0 mL). N-(3-Dimethylaminopropyl)-N′-ethylcarbodiimide hydrochloride (EDC, 1.92 g, 10 mmol), S-1-dodecyl-S′-(R,R′-dimethyl-R′′-acetic acid) trithiocarbonate (3.64 g, 10 mmol), and 4-dimethylamiopryidine (DMAP, 0.72 g, 6 mmol) were respectively added to the solution. Then the solution was cooled to 0 °C and then kept at 0 °C for ~ 30 minutes. Next, the reaction mixture was stirred for an additional 30 hours at room temperature to synthesize the RAFT agent modified silica nanoparticles. The nanoparticles were isolated by centrifugation at 5000 rpm, washed extensively with distilled water, methanol and acetone, and dried under vacuum at room temperature overnight.

Synthesis of poly(DEA-co-ProlA) functionalized silica nanoparticles. The synthesis of poly($DEA_{92.7}$-co-$ProlA_{7.3}$) grafted silica nanoparticles was employed to exemplify the preparation of the silica nanoparticle-supported polymeric catalyst. RAFT agent functionalized silica nanoparticles (0.9 g), DEA (4.62 g, 36 mmol), ProlA (1.1 g, 9 mmol), AIBN (10 mg, 0.06 mmol) and DMSO (24.0 mL) were added into a 50 mL Schlenk flask equipped with a magnetic stirrer. The mixture was degassed by three freeze–pump–thaw cycles, and then placed in a thermostated oil bath at 70 °C for 24 h. The polymerization was quenched in liquid nitrogen. Nanoparticles were isolated via centrifugation at 5000 rpm, redispersion in distilled water, and centrifugation again for four times. The obtained nanoparticles were dried in a vacuum oven overnight at 50 °C. The nanoparticles with different polymer compositions of the grafted layer were synthesized using the same method.

Aldol reaction in water. The nanoparticle-supported catalyst (18.2 mg, 2.3 mol%) was dispersed in a vial with 1.0 mL water, and then placed in an oil bath and stirred at 50 °C. In a second vial, a mixture of p-nitrobenzaldehyde (0.0232 g, 0.154 mmol, 1 eq.) and cyclohexanone (0.114 mL, 1.07 mmol, 7 eq.) was sonicated until p-nitrobenzaldehyde was fully dissolved. The reagents in the second vial were then added into the first vial (0.02 mL per 10 minutes). The reaction mixture was stirred for 24 hours. The reaction was quenched by cooling in an ice bath. The reaction mixture and 3 mL ethyl acetate were added to a small sample bottle and stirred extensively for 20 minutes. The organic phase was removed after 5 minutes of equilibrium. This process was repeated 3 times. The obtained organic phase was dried with $MgSO_4$ and concentrated under vacuum. The conversion and diastereoselectivity were determined by ^{1}H NMR spectroscopy with the crude aldol product. The crude aldol product was purified by silica gel column chromatography (Eluting with hexane/EtOAc 6:1) to give the aldol product as a colorless solid. The enantiomeric excess (ee) was determined by chiral-phase HPLC analysis.

The aldol reaction in aqueous solution in the presence of different types of ions was conducted using the same method. Specifically, the nanoparticle-supported catalyst (18.2 mg, 2.3 mol%) was dispersed

in a vial with 1.0 mL water, and the salt was added to the vial at the salt concentration of 1.7 M. After the salt was completely dissolved, the vial was placed in an oil bath and stirred at 30 °C for the following reaction.

Recycling of the catalyst. After the reaction was quenched, the aldol product was extracted using ethyl acetate, and then the aldol product was separated from the catalyst. The remaining phase with nanoparticles was transferred to the vial and the residual ethyl acetate and water were removed under vacuum. Then, 1.0 mL of water was added to the vial to re-disperse the nanoparticle-supported catalyst, and a second aldol cycle was carried out. The recycling of the catalyst was schematically illustrated in Scheme S1.

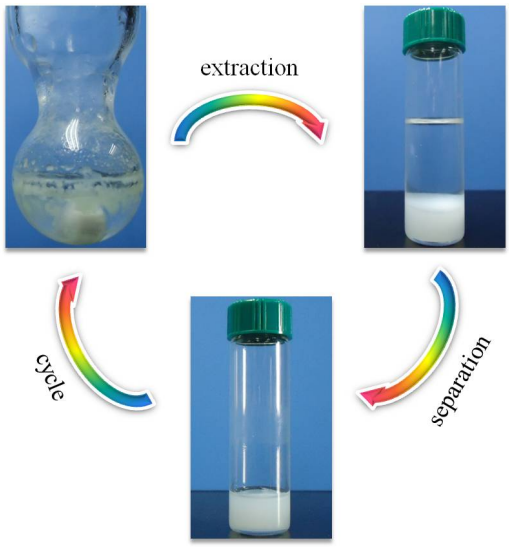

Scheme S1. Schematic illustration of the recycling of nanoparticle-supported catalyst.

Cleavage of the grafted copolymer from silica nanoparticles. Poly(DEA-co-ProlA) grafted silica nanoparticles (0.40g) were dispersed in an aqueous solution containing 1.0 M NaF in a PTFE vessel, and stirred at room temperature for 30 h. The solution was dialyzed against deionized water using a dialysis membrane (molecular weight cut off 1000) for 4 days. Afterwards, water was removed from the sample under vacuum and the recovered copolymer was analyzed by ^{1}H NMR.

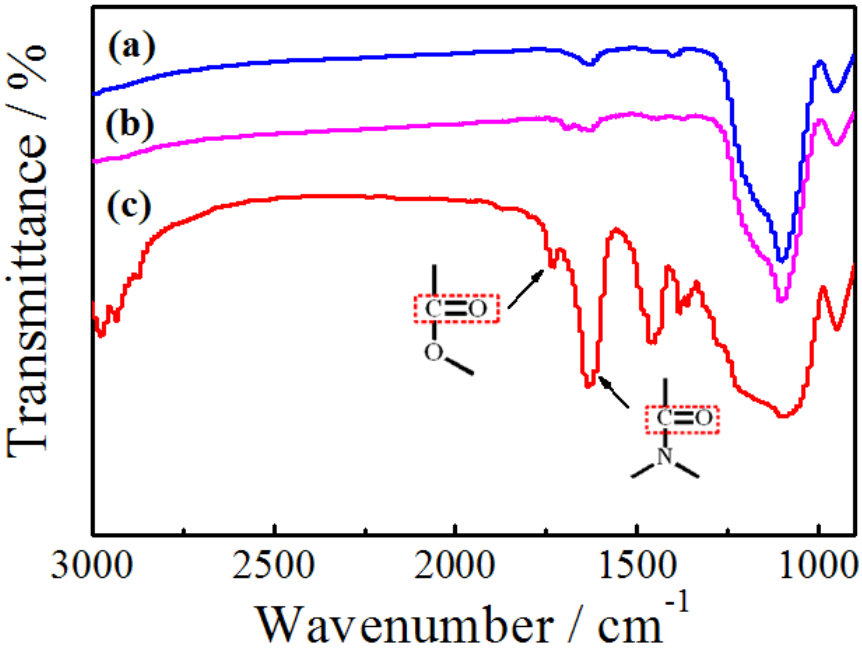

Figure S1. Fourier transform infrared (FT-IR) spectra of (a) bare silica nanoparticles, (b) RAFT agent functionalized silica nanoparticles and (c) poly($DEA_{92.7}$-co-$ProlA_{7.3}$) grafted silica nanoparticles.

In Figure S1c, the adsorption bands at 1628 cm^{-1} and 1732 cm^{-1} were ascribed to the stretching vibration of C=O bond for the -(C=O)N(C_2H_5)$_2$ group in DEA and the -(C=O)OR group in ProlA, respectively. This confirms the successful grafting of poly($DEA_{92.7}$-co-$ProlA_{7.3}$) onto the silica nanoparticles.

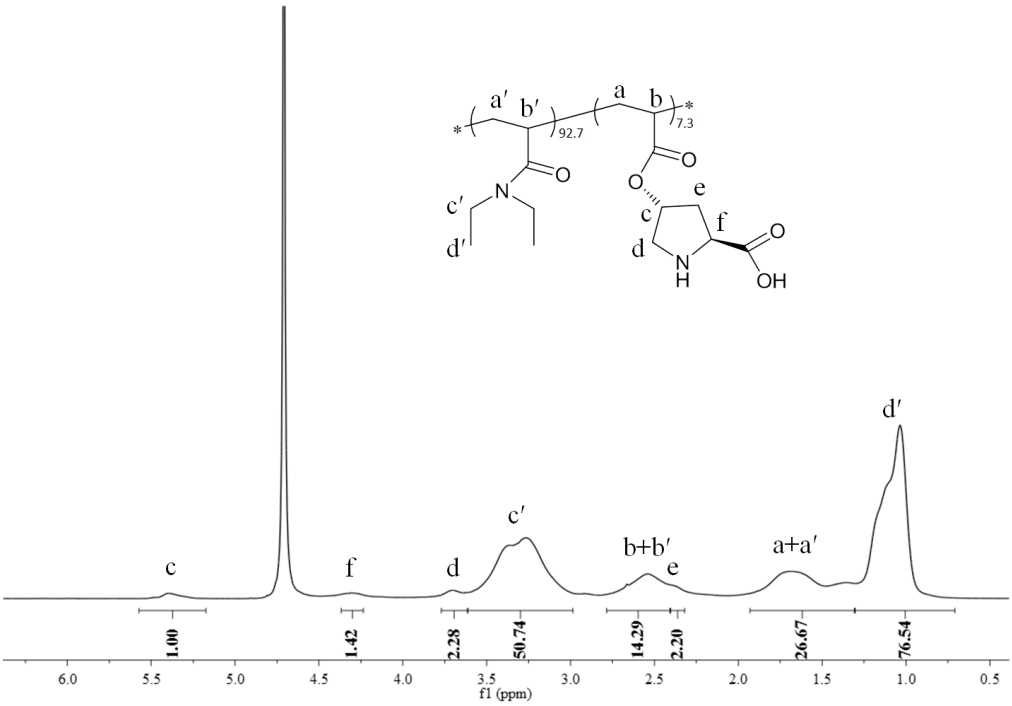

Figure S2. ^{1}H NMR spectrum of poly(DEA$_{92.7}$-co-ProlA$_{7.3}$) cleaved from the silica nanoparticles.

The composition of the grafted poly(DEA-co-ProlA) can be determined from the ^{1}H NMR spectrum of the copolymer cleaved from the silica nanoparticles as shown in Figure S2. This confirms the successful grafting of poly(DEA$_{92.7}$-co-ProlA$_{7.3}$) on the silica nanoparticles.

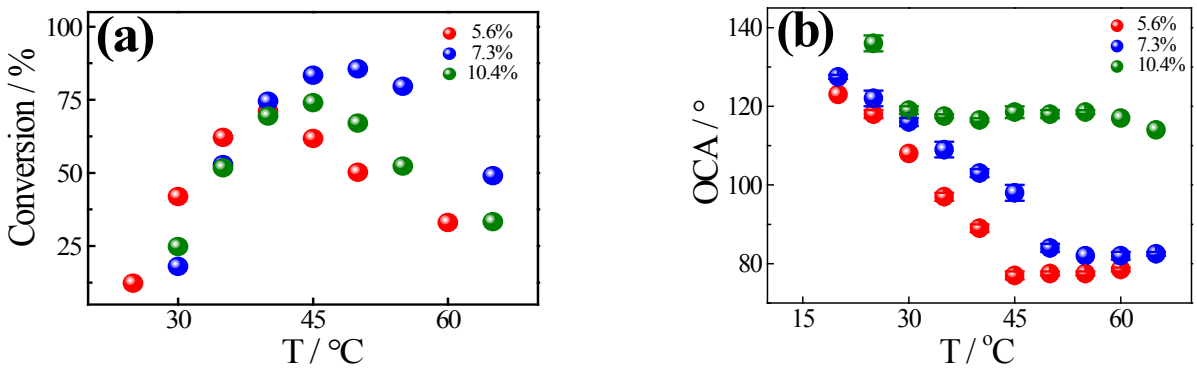

Figure S3. (a) Temperature dependence of change in catalytic efficiency of the as-prepared nanoparticle-supported organocatalysts as a function of the mole fraction of ProlA. (b) Temperature dependence of change in oil (cyclohexanone) contact angle (OCA) on the poly(DEA-co-ProlA) grafted silica surface as a function of the mole fraction of ProlA.

Among the catalysts with different polymer compositions, the catalyst with the content of PProlA of 7.3% exhibits the highest catalytic efficiency compared with the catalysts with either higher (10.4%) or lower (5.6%) content of PProlA. Details of the catalytic efficiency and selectivity are summarized in Table S1. The poly($DEA_{89.6}$-co-$ProlA_{10.4}$) grafted surface has a higher OCA than that of the poly($DEA_{92.7}$-co-$ProlA_{7.3}$) grafted surface. This means that the affinity between the catalyst and the substrate of the former is lower, leading to a lower catalytic efficiency. Alternatively, it has been reported that the local concentration of L-proline is important for the activity of the catalyst and a lower local concentration of L-proline gives rise to a lower catalytic efficiency.[S4] This may be why the catalyst with a PProlA content of 7.3% has a higher catalytic efficiency than that with a PProlA content of 5.6% even though the latter exhibits a higher affinity to the substrate at the same temperature. For this reason, the nanoparticle-supported catalyst with a PProlA content of 7.3% was employed as a model system to exemplify the modulation of performance of artificial organocatalyst by ion-specific effects.

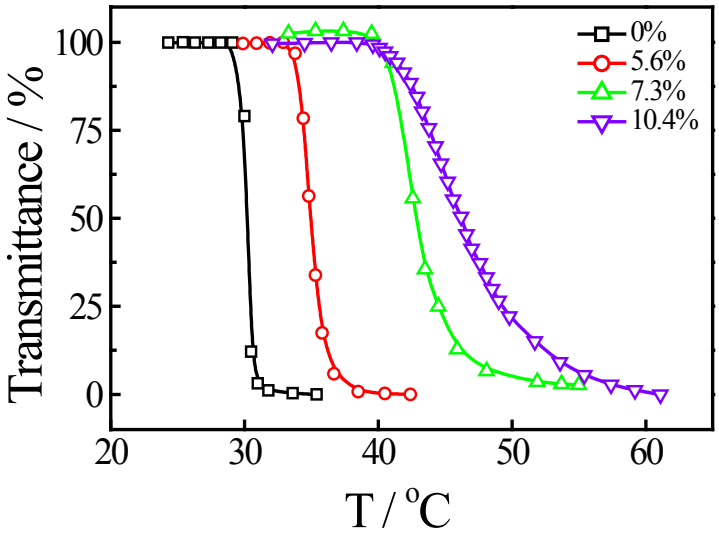

Figure S4. Temperature dependence of transmittance of poly(DEA-co-ProlA) solution (1.0 mg mL^{-1}) as a function of the mole fraction of ProlA. The phase transition temperature increases with increasing mole fraction of the hydrophilic ProlA.

In Figure S4, the LCST of poly($DEA_{92.7}$-co-$ProlA_{7.3}$) is ~ 44 ºC, close to the temperature at which the catalyst has the highest catalytic efficiency (Figure S3). Below the LCST, the affinity between the catalyst and substrate increases with temperature induced by increasing hydrophobicity of the polymeric organocatalyst, leading to an increase in catalytic efficiency with increasing temperature. Above the LCST, the direct disadvantageous temperature effect on the catalytic reaction itself would result in a decrease in catalytic efficiency with temperature where the hydrophobicity of the catalyst only weakly changes with temperature. Thus, there might be a correlation between LCST and catalytic efficiency.

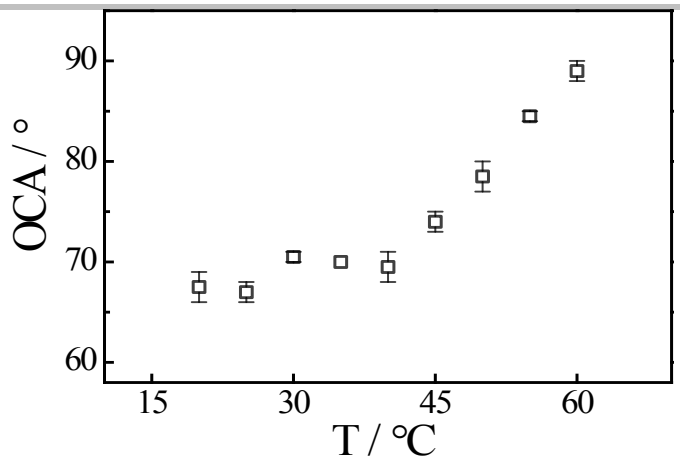

Figure S5. Oil (cyclohexanone) contact angle on the RAFT agent modified silica surface as a function of temperature.

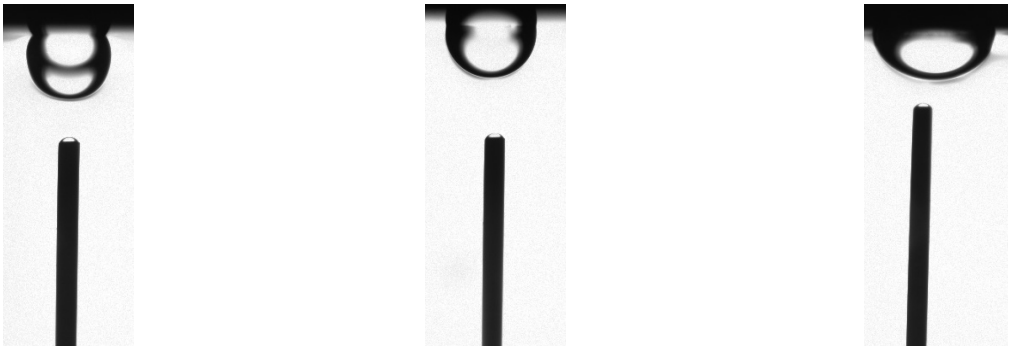

T = 20 ºC, OCA = 128º, contact area ~ 1.09 mm^2 **(a)**

T = 45 ºC, OCA = 98º, contact area ~ 1.65 mm^2 **(b)**

T = 65 ºC, OCA = 83º, contact area ~ 3.23 mm^2 **(c)**

Figure S6. Photos for the oil (cyclohexanone) droplet contacting on the poly($DEA_{92.7}$-co-$ProlA_{7.3}$) grafted surface as a function of temperature. (a) 20 ºC, (b) 45 ºC, and (c) 65 ºC.

In Figure S6, a 4 μL droplet of cyclohexanone (reactant) is employed to investigate the accessibility of the reactant to the polymeric catalyst grafted surface. The underwater oil contact angle (OCA) decreases from 128º to 83º as the temperature increases from 20 ºC to 65 ºC, implying that the affinity between the catalyst and the reactant is enhanced as the adhesive force between the droplet and the surface is inversely related to the OCA. Meanwhile, the contact area between the droplet and the surface increases from 1.09 mm^2 to 3.23 mm^2 with increasing temperature from 20 ºC to 65 ºC, indicating that the catalyst is more accessible for the reactant with increasing temperature due to the enhanced affinity.

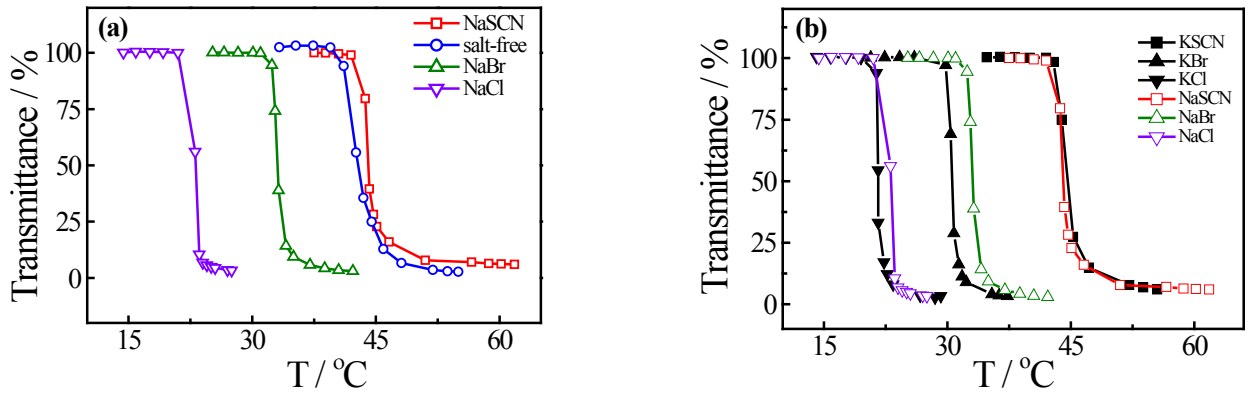

Figure S7. (a) Temperature dependence of transmittance of poly($DEA_{92.7}$-co-$ProlA_{7.3}$) solution in the presence of different types of anions with Na^+ as the common cation. (b) Comparison of temperature dependence of transmittance of poly($DEA_{92.7}$-co-$ProlA_{7.3}$) solution between the sodium salts and the potassium salts. Here, the polymer concentration is fixed at 1.0 mg mL^{-1} and the salt concentration is fixed at 1.7 M.

In Figure S7a, the LCST of the polymeric catalyst increases following the series Cl^- < Br^- < salt-free < SCN^-, suggesting that Cl^- and Br^- exhibit a salting-out effect but SCN^- has a salting-in effect. In the presence of 1.7 M SO_4^{2-}, no LCST of the copolymer was detected before the precipitation of Na_2SO_4 or K_2SO_4 due to decreasing temperature. This indicates that the SO_4^{2-} has the strongest salting-out effect among the anions. Since the catalytic efficiency is correlated with the LCST of the polymeric catalyst (Figure S4) and the LCST can be modulated by the anions, the anion-specific catalytic efficiency domonstrated in this work could also be understood based on the modification of LCST of the polymeric catalyst by the added anions.

In order to examine how ion-pairing would influence the anionic effect on the hydrophobic interactions of the polymeric catalyst, we have compared the temperature dependence of transmittance of poly($DEA_{92.7}$-co-$ProlA_{7.3}$) solution between the sodium salts and the potassium salts (Figure S7b). In comparison with Na^+, K^+ is a more chaotropic (weakly hydrated) cation. Therefore, the K^+ has different ability to form ion pair with the anions in solution according to the model of matching water affinities.[S5] However, the LCST of the polymeric catalyst only has a small change (~ 1-2 ºC) when the cation changes from Na^+ to K^+ with the common anion. This result indicates that the ion-pairing may only have a weak influence on the anionic effect on the hydrophobic interactions of the polymeric catalyst.

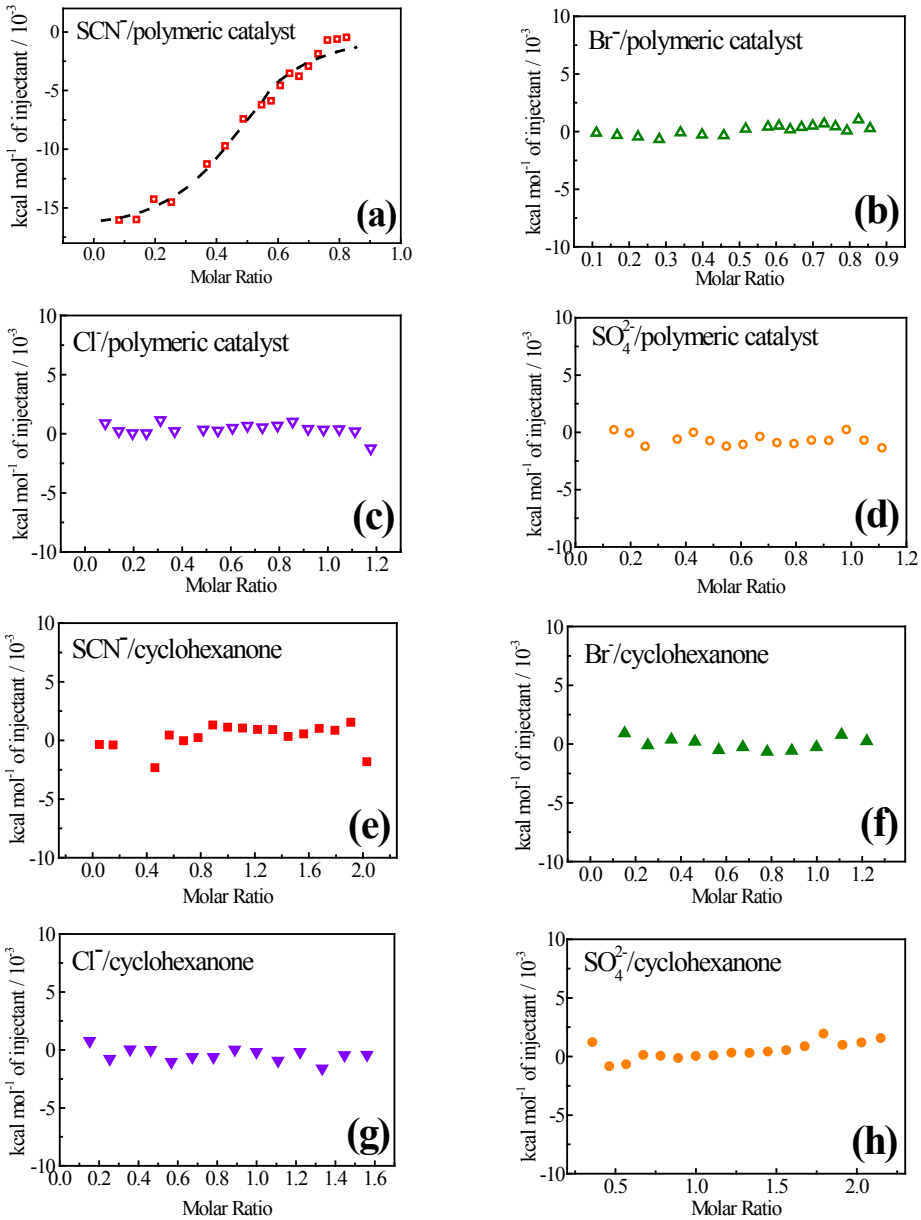

Figure S8. ITC titration data derived from the integrated heat of the exothermic peaks for the titration of salt solutions into catalyst solution (a, b, c, d) and cyclohexanone solution (e, f, g, h). SCN^-: (a) and (e), Br^-: (b) and (f), Cl^-: (c) and (g), SO_4^{2-}: (d) and (h). Here, the ionic strength of the salt solutions is fixed at 0.1 M, the concentration of polymeric catalyst is fixed at 2.5 mg/mL, and the concentration of cyclohexanone is fixed at 1.0 mg/mL.

For the polymeric catalyst, the isothermal titration calorimetry (ITC) results show that only SCN^- can bind onto the catalyst surface, whereas other types of anions including Br^-, Cl^- and SO_4^{2-} exhibit no obvious binding on the catalyst surface (Figure S8 a-d). The binding constant of SCN^- to the catalyst is 1.73×10^3 M^{-1} obtained by fitting the titration data. The direct binding of SCN^- to the catalyst gives rise to a salting-in effect, as reflected by a higher LCST of the polymeric catalyst in the presence of SCN^- compared with the salt-free solution (Figure S7). The salting-in effect exerted by SCN^- would generate a more hydrophilic environment around the catalyst, thereby reducing the affinity between the catalyst and the reactants. For the reactants, p-nitrobenzaldehyde is in solid state and is insoluble in water. Therefore, it is not possible to study the binding of anions to p-nitrobenzaldehyde using ITC method. Cyclohexanone is slightly soluble in water. Our ITC results show that all the anions exhibit no obvious binding to cyclohexanone molecules (Figure S8 e-h). Thus, the direct anion binding effect on the reactants might be very weak.

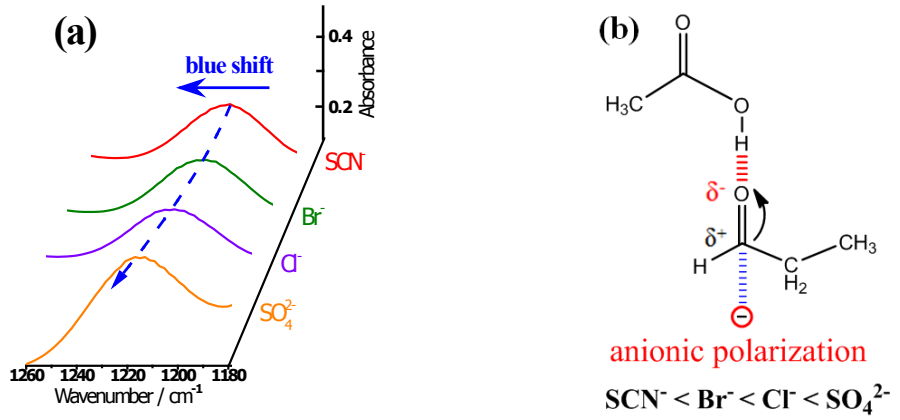

Figure S9. (a) Fourier transform infrared (FT-IR) spectra of the propionaldehyde-acetic acid mixture in D_2O in the presence of different types of anions in the frequency range of 1180 to 1260 cm^{-1}. (b) Schematic illustration of the modulation of hydrogen bonding between propionaldehyde and acetic acid via anionic polarization. Here, 10 µL of propionaldehyde and 10 µL acetic acid were added to 100 µL D_2O for the FTIR experiments. The salt concentration was fixed at 1.7 M.

In Figure S9a, the 1210 cm^{-1} spectral peak corresponds to the $-CH_2-$ twist motion of propionaldehyde. The peak shifts to higher frequency from ~1206 cm^{-1} to ~1215 cm^{-1} as the anions change from the chaotropic SCN^- to the kosmotropic SO_4^{2-}. A stronger hydrogen bond between the carboxylic acid group on acetic acid and the carbonyl group on the propionaldehyde would generate a stronger electron withdrawing effect on the $-CH_2-$ twist motion (Figure S9b), causing the spectral peak to shift to higher frequency. In other words, the blue shift of the spectral peak as the anions change from SCN^- to SO_4^{2-}, indicating that the hydrogen bonding between the carboxylic acid group and the carbonyl group is strengthened following the series $SCN^- < Br^- < Cl^- < SO_4^{2-}$ induced by the anionic polarization. This result supports our proposed mechanism that a more kosmotropic anion can more effectively strengthen the hydrogen bonding and stabilize the transition state via anionic polarization.

Besides, the salt induced change of LCST might also play a role in the stabilization of transition state. The LCST of the polymeric catalyst in the presence of anions decreases following the series $SCN^- > Br^- > Cl^- > SO_4^{2-}$, suggesting that the polymeric catalyst becomes more hydrophobic as the anions change from SCN^- to SO_4^{2-} along the series. Therefore, the catalyst would exhibit stronger hydrophobic interactions with the substrate in the presence of a more kosmotropic anion, which is more favorable for the stabilization of the transition state.

Thus, the higher catalytic efficiency for Br^- compared with that for the salt-free solution may also include the contribution from the salting-out effect exerted by Br^-, as the LCST of the polymeric catalyst in the presence of Br^- is lower than that of the salt-free solution induced by the increase in surface tension of the water/polymer interface with the addition of Br^- (Figure S7), similar to the previsous studies on poly(N-isopropylacrylamide) and poly(diethylacrylamide).[S6,S7]

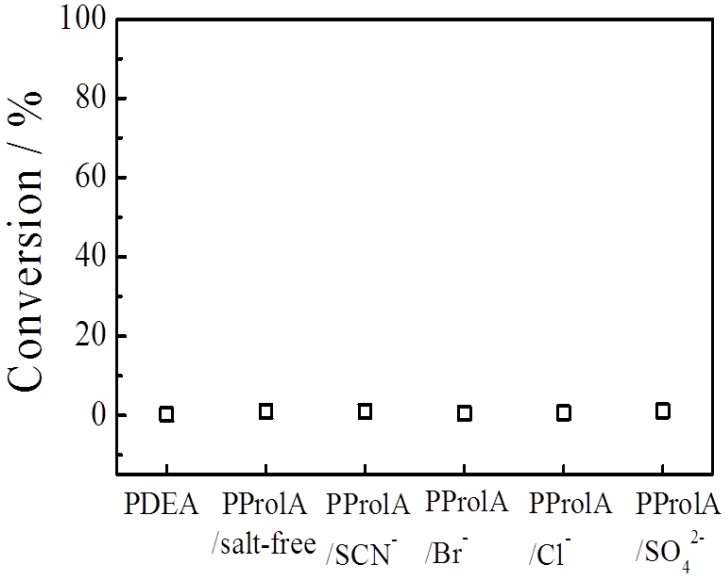

Figure S10. Conversion of the aldol reaction in the presence of PDEA (M_n ~ 8.3×10^4 g/mol) or in the presence of PProlA (M_n ~ 4.0×10^3 g/mol) with different anions, where the salt concentration is fixed at 1.7 M. This demonstrates that either the pure PDEA or the PProlA in the presence of the anions cannot catalyze the aldol reaction.

Table S1. Catalytic data for the aldol reaction of cyclohexanone and p-nitrobenzaldehyde catalyzed by the nanoparticle-supported catalyst of poly(DEA-co-ProlA) with different contents of ProA at 2.3 mol % catalyst loading.

5.6% (mol/mol)				7.3% (mol/mol)				10.4% (mol/mol)			
T / °C	conv.%	anti/syn	ee%	T / °C	conv.%	anti/syn	ee%	T / °C	conv.%	anti/syn	ee%
25	12	92/8	93	30	18	90/10	90	30	25	80/20	94
30	42	92/8	97	35	53	82/18	94	35	52	67/33	95
35	62	93/7	95	40	75	89/11	95	40	69	85/15	96
40	71	92/8	97	45	83	83/17	94	45	74	81/19	95
45	62	84/16	92	50	85	86/14	94	50	67	76/24	92
50	50	85/15	93	55	80	83/17	93	55	52	88/12	89
60	33	73/27	70	65	49	73/27	83	65	33	73/27	70

References

S1. Lai, J. T.; Filla, D.; Shea, R. *Macromolecules* 2002, **35**, 6754-6756.
S2. Yacob, Z.; Nan, A.; Liebscher, J. *Adv. Synth. Catal.* 2012, **354**, 3259-3264.
S3. Stober, W.; Fink, A.; Bohn, E. *J. Colloid Interface Sci.* 1968, **26**, 62-69.
S4. Huerta, E.; Stals, P. J. M.; Meijer, E. W.; Palmans, A. R. A. *Angew. Chem. Int. Edit.* 2013, **52**, 2906-2910.
S5. Collins, K. D. *Methods* 2004, **34**, 300-311.
S6. Zhang, Y. J.; Furyk, S.; Bergbreiter D. E.; Cremer, P. S. *J Am Chem Soc*, 2005, **127**, 14505-14510.
S7. Rembert, K. B.; Okur, H. I.; Hilty, C.; Cremer, P. S. *Langmuir* 2015, **31**, 3459-3464.